IEEE Robotics and Automation Letters (RA-L) paper, presented at ICRA 2024, Yokohama, Japan. Cite as RA-L paper.

A Bio-plausible Approach to Realizing Heat-evoked Nociceptive Withdrawal Reflex on the Upper Limb of a Humanoid Robot

Fengyi Wang[1], J. Rogelio Guadarrama Olvera[1], Nitish Thakor[2] and Gordon Cheng[1]

***Abstract*—In this letter, we present a method for realizing the heat-evoked nociceptive withdrawal reflex (NWR) in the upper limb of a humanoid robot so that it can avoid the potential damage caused by noxious heat. We use a spiking neural network whose structure, encoding scheme, and form of information transmission mimic the reflex arc in humans to improve bio-plausibility. The proper synaptic strengths between the sensory neurons and the interneurons in the first two layers are learned using the bio-plausible reward-modulated spike timing-dependent plasticity learning algorithm. By monitoring the spikes from the motor neuron in the third layer, a reflex matching the intensity of the stimulation can be evoked. Experimental evaluations show that noxious heat stimulation can be detected online and evoke the NWR. The experiments on a full-size humanoid robot show that the method enables robots to avoid potential damage robustly with proper NWR, depending on the site and intensity of the stimulation. We also verify that the method takes advantage of the intrinsic characteristics of its neuromorphic encoding scheme to reproduce essential features of the NWR, e.g., spatial summation effect and temporal summation effect in humans. The improved bio-plausibility and the capability to reproduce the human-like feature.**

I. Introduction

The capability to interact with environments that are not fully known and avoid potential damage is vital for the safe operation of robots. Many mechanisms have been used to protect robots from damage caused by mechanical collisions while preventing damage caused by external heat has received less attention. For example, when a robot works in an environment where high-temperature heat sources exist, e.g., a kitchen with a stove, it should quickly move the parts that are too close to the heat source before they are damaged.

The human reaction under noxious stimulation provides an excellent example for humanoid robots to learn from. We can transfer knowledge about human behavior to robotic systems to provide robots with human-like interaction mechanisms. On the other hand, humanoid robots provide us with the flexibility to quantify the reflexive behaviors of robotic devices before being tested on a prosthesis involving the human body. Recently developed neural prosthesis intends to provide perceptual feedback to amputees [1]. It demands local data processing with low energy consumption and the transmission of the processed data over constrained channels to the human user. Such performance can be achieved by means of novel forms of information representation and processing, such as neuromorphic algorithms like spiking neural networks (SNNs). The development of event-driven robot skins [2] and of neuromorphic processors like Intel's Loihi 2 [3] opens a perspective to mimic the fast and robust nature of reflex under a low energy budget.

In this paper, we present a bio-plausible approach based on SNN to realizing the nociceptive withdrawal reflex on the upper limb of a humanoid robot. The neuromorphic NWR system is illustrated in Fig. 1.

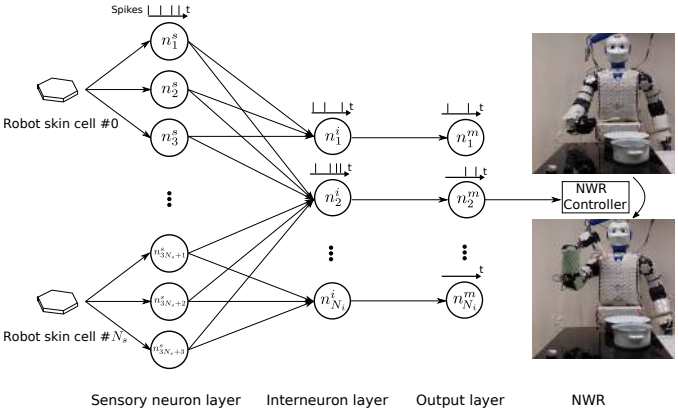

Fig. 1: Illustration of the proposed heat-evoked NWR system that involves N_s robot skin cells, N_i interneurons, and N_i motor neurons.

A. Nociceptive withdrawal reflex evoked by heat

The nociceptive withdrawal reflex (NWR) is a polysynaptic spinal reflex that protects the body from damaging stimulation. The NWR evoked by stimulation of a certain skin area can be defined as a movement perpendicular to the skin surface away from the stimulation site [4]. It withdraws the affected skin site from the noxious stimulation to avoid potential damage while the body maintains balanced [5].

Proper reaction of the external stimulation relies on faithful encoding by sensory neurons. [6] shows that not only the response of an individual neuron is increased monotonically, but also more neurons are activated as the increase of intensity of the heat stimulation. Since primary afferents have different encoding strategies for cold and heat. Thus, this work focuses only on the reaction to heat stimulation.

The evoke of NWR is not simply gated by a fixed temperature threshold but a consequence of the excitability of

Manuscript received: October, 24th, 2022; Revised January, 18th, 2023; Accepted: April, 8th, 2023.

This paper was recommended for publication by Editor Abderrahmane Kheddar upon evaluation of the Associate Editor and Reviewers' comments. This work was supported by the German Federal Ministry of Education and Research (BMBF)

[1]Fengyi Wang , J. Rogelio Guadarrama Olvera, and Gordon Cheng are with the Institute for Cognitive Systems, Technical University of Munich, Arcisstrae 21, 80333 Munich, Germany { fengyi.wang, rogelio.guadarrama, gordon } @tum.de

[2]Nitish Thakor is with the Department of Biomedical Engineering, Johns Hopkins University, Baltimore, MD, USA nitish@jhu.edu

Digital Object Identifier (DOI): see top of this page.

IEEE Robotics and Automation Letters (RA-L) paper, presented at ICRA 2024, Yokohama, Japan. Cite as RA-L paper.

spinal reflex arch, descending control, and the current sensory input [7]. High-intensity stimulation or concurrent inputs from multiple sites can activate more sensory neurons and thus enhance or facilitate the NWR. This phenomenon is known as the spatial summation effect [8]. Another phenomenon is the temporal summation effect, i.e., the withdrawal reflex can be evoked by high-frequency stimulation with a sub-threshold intensity [9].

The input signals from different sites over time converge in the interneurons in the spinal cord [7]. The interneurons also encode the withdrawal reflex strength and project the output to motor neurons [10].

B. Neuromorphic NWR system

SNN mimic natural neural networks more closely. In SNN, neurons only transmit information via action potentials (spikes) when the membrane voltage reaches the threshold. Thus, SNN can save a large amount of energy used for data transfer in artificial neural networks to support more powerful computations with less energy consumption, especially when implemented on neuromorphic chips [11].

One of the most biologically plausible spiking neuron models is the Hodgkin-Huxley model [12]. However, it is computationally heavy and has tens of parameters, making it difficult to tune. In contrast, another widely used model, the leaky integral firing (LIF) model, is so simplified that it cannot reproduce the firing pattern of biological neurons. In this work, we consider the Izhikevich model that is computationally efficient but can still reproduce all the mutually exclusive properties of biological neurons [13].

Spiking neurons have been used to detect touch and pain online [1]. Nevertheless, it can only make a binary classification between a noxious and innocuous stimulation rather than assess the intensity of the stimulation and generate corresponding responses. The lack of a training algorithm makes the model rely on manually tuned parameters.

C. Contribution

Using our robot skin [2], the environmental temperature can be acquired from every part of a humanoid robot. In this paper, we propose a neuromorphic model that mimics the reflex arc in terms of the structure, encoding scheme at individual and population levels, and the information transmission method between neurons. We designed a bio-plausible reward-modulated spike timing dependent plasticity algorithm to enable the network to assess the intensity of external stimulation and generate the corresponding output signal online. The proposed method utilizes the intrinsic characteristics of SNN and neuromorphic encoding scheme to reproduce several essential features of the NWR in humans without additional modeling or training. Our neuromorphic approach may help build closed-loop interfaces with suitable feedback to human users, which remains a challenge [14]. The NWR controller generates an appropriate reaction motions in robots. We demonstrate the capability of a humanoid robot (H1) [2], [15] to detect noxious heat stimulation while moving its upper limb and prevent potential damage caused by heat with NWR while its body maintains stable and balanced.

II. Methodology

A. Environmental temperature measurement

Each robot skin cell is a sensing unit that can measure external stimulation of different modalities, including temperature. In addition, the robot skin also provides information about its position, so the stimulation can be well located.

The area of the robot body where the stimulation is expected is covered with robot skin. With the event-driven communication architecture with an event threshold 0.09375 °C, the robot skin can deliver sensing information on a large scale at up to 250 Hz.

B. Bio-mimetic spiking neural networks

1) Sensory neuron layer: The temperature measured by the robot skin is encoded into spike trains in real-time by Izhikevich neurons [16]. The internal states are described with the following equations:

$$\begin{cases} dv_i/dt = 0.04{v_i}^2 + 5v_i + 140 - u_i + I \\ du_i/dt = a(bv_i - u_i) \end{cases} \tag{1}$$

$$\text{if } v_i \geq v_{th}^s, \text{ then} \begin{cases} v_i \leftarrow c \\ u_i \leftarrow u_i + d \end{cases} \tag{2}$$

The dynamic of a neuron is defined by four parameters a,b,c, and d. The variable v_i represents the membrane potential of the artificial sensory neuron n_i^s. The variable I describes the polarization rate caused by external stimuli, having a unit of mV/ms. When v_i reaches the threshold v_{th}^s, the neuron spikes, and the v_i is reset to c. u_i is the membrane recovery variable that increases by d when the sensory neuron n_i^s spikes.

Heat stimulation induces an initial burst activity and subsequent adaptation to stable temperature in heat-sensitive neurons [17]. So we adopt the parameters of the Izhikevich neuron model with the intrinsically bursting spiking pattern to mimic the firing pattern of the biological heat-sensitive neurons where $a = 0.02$ ms^{-1}, $b = 0.2$ ms^{-1}, $c = -55$ mV, $d = 8$ mV/ms and $v_{th} = 30$ mV.

Biological heat-sensitive neurons have different activation temperatures T_a, and the response of the vast majority of them increases monotonically with increasing intensity of the heat stimulation in a half Gaussian-like form [6]. Thus, we use functions (3) and (4) to mimic such tuning curve:

$$I_i^s = \exp\left(-\frac{1}{2}\frac{(T_{max}^i - T)^2}{\sigma_i^2}\right) \cdot I_{max}^s \tag{3}$$

$$\text{if } T \geq T_{max}^i, \text{ then } I_i^s = I_{max}^s \tag{4}$$

I_i^s represents the polarization rate of the i-th sensory neuron n_i^s whose activation temperature is T_a^i. T represents the temperature of the robot skin sensor, and T_{max}^i is the temperature at which n_i^s is fully activated. T_{max} is set to 52 °C for all n_i^s according to the activation threshold of the TRPV2 ion channel, which is related to the detection of very hot temperature (> 52 °C). $\sigma_i = T_{max} - T_a^i$, so that all neurons have the same polarization rate I_a^s at their respective activation temperatures:

$$I_a^s = e^{-\frac{1}{2}} \cdot I_{max}^s \tag{5}$$

We set I^s_{max} to 20 mV/ms, so that step response of polarization rate I^s_a causes burst activity. Otherwise, the neuron spikes regularly as the ongoing activity in the biological heat-sensitive neurons [18].

Furthermore, [6] showed that heat is also encoded in a graded fashion by a population of neurons, which means that more heat-sensitive neurons are activated as temperature increases. There are mainly three groups of heat-sensitive sensory neurons whose activation temperatures are T_a = 38 °C, 43 °C and 50 °C, respectively. According to this mechanism, three artificial sensory neurons with the corresponding activation temperatures are used to perform the neuromorphic encoding at the population level.

2) Interneuron layer: The interneurons in primates also have a burst firing pattern [19]. We use the same neuron model (1) (2) to describe the internal states of interneurons.

The spike trains from a skin cell and its neighbors, and the descending control converges in the interneuron layer. The polarization rate of an interneuron is increased when it receives a spike from a sensory neuron. Otherwise, the polarization rate decreases over time.

The amplitude of the post-synaptic polarization rate change can be determined by the synaptic strengths $s_{i,j}$ between the i-th sensory neuron n^s_i and the j-th interneuron n^i_j. We use a parameter ϵ to represent the overall effect of the descending control and the excitability of the spinal reflex arch. The polarization rate of the j-th interneuron I^i_j is described by the following equation:

$$dI^i_j/dt = -I^i_j/\tau_i \tag{6}$$

$$\text{when } n^s_i \text{ spikes, } I^i_j = I^i_j + \epsilon \cdot s_{i,j} \cdot I_{max} \tag{7}$$

The robot skin cells mounted on the same part of the robot are considered homogeneous, and all the corresponding sensory neurons contribute to the membrane potential of the interneuron. Thus, the overall excitability E of the neuromorphic model for these N_s cells is:

$$E = N_s \cdot \epsilon \tag{8}$$

While $E = 1$ is the normal state, $E > 1$ means that the NWR is facilitated, and $E < 1$ means that the NWR is inhabited. The synaptic strengths $s_{i,j}$ are determined with the learning algorithm introduced in II-C.

3) Output layer: This layer contains several artificial motor neurons n^m_i that mimic an α motor neuron that evokes the NWR in humans. These neurons can be modeled as leaky integrate and fire neurons with synapses connected to the interneurons [1]. The dynamic of the motor neurons can be described with the following equations:

$$dv_m/dt = (v_0 - v)/\tau_m \tag{9}$$

$$\text{if } v_m \geq v^m_{th}, \text{ then } v_m = v_0 \tag{10}$$

The resting potential v_0 = -70 mV and the time constant τ_m = 50 ms which is presented in [20]. A spike from an interneuron induces a 30 mV increment in the membrane potential of the motor neuron v_m. When v_m reaches the threshold v^m_{th}, the motor neuron generates a spike, and the membrane potential v_m is reset to the resting potential v_0.

C. Learning algorithm

The network's response is evaluated after the stimulation phase. The patterns may no longer be there when the reward comes, making it a distal reward problem. The ongoing activity of the sensory neurons may also affect the determination of the proper synaptic strengths of synapses. These problems can be solved with the bio-plausible reward-modulated spike timing dependent plasticity (R-STDP) algorithm. In this work, the synaptic strengths of the synapses between the sensory neurons and the interneurons are determined with the R-STDP algorithm [20].

In an STDP synapse, the modification of synaptic strength $s_{i,j}$ that arises from a pair of pre- and post-synaptic spikes with the inter-spike interval $\Delta t = t_{post} - t_{pre}$ is expressed by $F(\Delta t)$:

$$F(\Delta t) = \begin{cases} \mathrm{A}_+ \exp\left(\Delta t/\tau_+\right) \text{ if } \Delta \mathrm{t} < 0 \\ \mathrm{A}_- \exp\left(-\Delta t/\tau_-\right) \text{ if } \Delta \mathrm{t} \geq 0 \end{cases} \tag{11}$$

The reward modulation of an STDP synapse can be described by the following differential equations:

$$\begin{cases} dC/dt = -C/\tau_C \\ de/dt = -e/\tau_e + F(\Delta t) \cdot \delta(t_{pre/post}) \\ ds/dt = C \cdot e/\tau_s \end{cases} \tag{12}$$

The variable C represents the concentration of extracellular dopamine, i.e., the reward/punishment signal, and e represents the eligibility trace for synaptic modification. The decay rates τ_C, τ_e, and τ_s control the sensitivity of the plasticity to the delayed reward/punishment.

Previous research has demonstrated that the NWR threshold is often highly correlated with the pain threshold and that the NWR magnitude is related to the intensity of perceived pain level [21], [22]. The relationship between the intensity of perceived pain and the intensity of the stimulation is: $\psi = \mathbf{k}\left(T - T_0\right)^\alpha$, where T is stimulation intensity (temperature) and T_0 is the threshold of pain [8]. We define the normalized perceived pain level $|\psi|$ as the ratio of the pain intensity to the pain intensity at T_{max}:

$$|\psi| = \frac{\psi}{\psi_{max}} = \frac{\mathbf{k}\left(T - T_0\right)^\alpha}{\mathbf{k}\left(T_{max} - T_0\right)^\alpha} = \left(\frac{T - T_0}{T_{max} - T_0}\right)^\alpha \tag{13}$$

$|\psi|$ is independent of the scaling factor k. $\alpha = 2.3$ and $T_0 = 44$ °C according to [8].

In the learning phase, the motor neuron does not fire so that a continuous membrane potential v_m can be obtained. v_m is normalized by a scaling factor K to match the scale of $|\psi|$ and the threshold of the motor neuron:

$$|v_m| = (v_m + v^m_{th})/K \tag{14}$$

Ideal noxious stimulations of random intensities that lasts for 100 ms followed by a cooling phase that lasts for 2 seconds at the baseline temperature are presented to the network. The baseline temperature is 35 °C in this learning algorithm, which is the same as the experiments in [8][23]. The maximum value of the average membrane potential $|v_m|_{max}$ during the stimulated phase is defined as the activation level of the motor neuron.

An noxious step stimulation with magnitude T_s applied on time t_0 and last for t_s is defined as:

$$T = T_s \cdot (H(t - t_0) - H(t - t_0 - t_s)) \tag{15}$$

where the magnitude $T_s \geq T_0$ and $H(t)$ is the Heaviside step function.

After each stimulation phase, a reward/punishment signal is given. The intensity of the reward/punishment is determined by the relationship between the normalized perceived pain level $|\psi|$ and the activation level $|v_m|_{max}$.

$$C = |\psi| - |v_m|_{max} \tag{16}$$

The parameters used for the learning algorithm are summarized in table I.

An example of the learning process using the R-STDP algorithm is illustrated in Fig. 2.

D. NWR in the upper limb of the robot

When the stimulation is strong enough, the NWR in the upper limb of the robot is evoked to avoid potential damage. Based on the results of previous studies in animals [4], we define the NWR evoked by stimulation of a certain robot skin area in robots as a movement perpendicular to the skin surface away from the stimulation site in Cartesian space. The average temperature $\bar{T_R}$ of the affected skin cells at which the NWR is evoked is defined as the NWR threshold.

The strength of the NWR is determined by the reflex gain g_r encoded by the relative spike latency Δt between spikes of the motor neuron

$$g_R = 1 + exp(\frac{\Delta t_{min} - \Delta t}{K_m}) \tag{17}$$

We set $\Delta t_{min} = 45$ ms according to the response to step stimulation at 50 °C. The scaling factor K_m is set to 20. When $\Delta t > 100$ ms, we consider the stimulation too weak to evoke

TABLE I: Parameters used in learning algorithm

A_+	A_-	τ_+	τ_-	τ_C	τ_e	τ_s	K
0.1	0.1	20 ms	20 ms	100 ms	200 ms	5 ms	150 mV

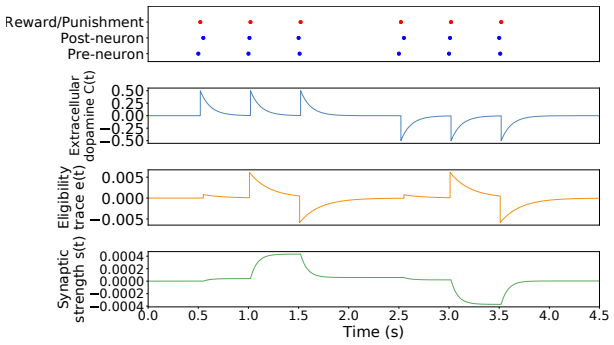

Fig. 2: In (a), the red and blue dots represent the time when the reward/punishment signal are given and when the post- and presynaptic neurons spike, respectively. (b), (c) and (d) show important variables in the R-STDP.

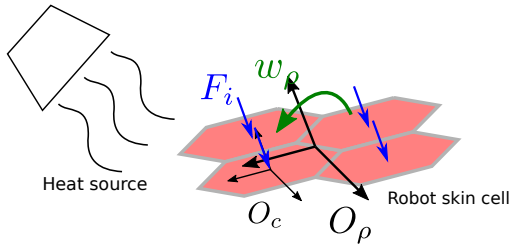

Fig. 3: Patch wrench w_R generation with robot skin.

an NWR. The magnitude of the virtual reflex force vector F_i depends on the reflex gain g_R:

$$F_i = [0, 0, g_R \cdot f]^\top \tag{18}$$

The stimulation site is obtained from the robot skin. Then, we can define a coordinate frame O_c where the center of a skin cell is located. O_ρ is defined as the common reference frame of the affected skin cell and its neighboring cells. F_i is applied perpendicularly to these cells to generate the NWR.

The cell wrench $w_{i\rho}$ in O_ρ is then computed

$$w_{i\rho} = \begin{bmatrix} {}^\rho R_i F_i \\ {}^\rho p_i \times {}^\rho R_i F_i \end{bmatrix} \tag{19}$$

where ${}^\rho R_i \in SO(3)$ is the rotation from O_c to O_ρ, and ${}^\rho p_i \in R^3$ is the translation from the origin of O_c to O_ρ.

The patch wrench w_R used in the torque computation is the accumulation of cell wrenches:

$$w_R = \sum_{i=1}^{N_s} w_{i\rho} = \begin{bmatrix} F_R \\ \mu_R \end{bmatrix} \tag{20}$$

With the transformations from O_ρ to the base link O_0, the joint torque vector $\tau_R \in \mathbf{R}^n$ generated by w_R is computed:

$$\tau_R = {}^0 J_\rho^\top(q) w_R \tag{21}$$

where τ_R is the joint torque vector generated by the virtual reflex force, and ${}^0 J_\rho \in \mathbf{R}^{6\times n}$ is the geometric Jacobian mapping joint velocities $\dot{q}$ onto Cartesian velocities of O_ρ with respect to the world coordinate frame O_0.

The humanoid robot is a floating base system with naturally unstable and constrained dynamics. Thus, the NWR controller has to be executed alongside other controllers, e.g., the center of mass controller and self-collision avoidance controller, to produce intelligent behaviors in a humanoid robot. The robot runs a strict hierarchical control system using the null-space projection method [24] to guarantee the bipedal balance and postural stability. For a free-floating base system in the form

$$M(x)\dot{\nu} + C(x, \nu)\nu + g(x) = S^\top \tau \tag{22}$$

where x is the state vector containing the pose of the floating base and the joint states. $\nu \in \mathbf{R}^{n+6}$ is the complete velocity coordinates, containing the floating base's linear and rotational velocities and joint velocities. $M(x), C(x, \nu)$ and $g(x)$ are the inertia matrix, Coriolis matrix, and gravity effects vector, respectively.

The NWR controller is executed in the null space of controllers with higher priority as described in [25]. The control of the system is computed in the form:

$$\tau = \tau_{const} + N_{const}\left(\tau_1 + N_2\left(\tau_2 + \ldots + N_m\tau_m \ldots\right)\right) \quad (23)$$

where τ_{const} is the torque vector generated by the constraints and highest priority tasks, and N_{const} is the dynamically consistent null-space projector to execute the lower priority tasks in the null-space of the constrained tasks and N_m represents the null-space projector for the controller with the m-th priority.

In this work, the priority of the NWR task is lower than the tasks that guarantee the biped balance of the humanoid robot but higher than the purpose tasks such as the Cartesian hand task.

III. Experimental evaluation

In these experiments, responses of the proposed neuromorphic model to stimulated and realistic heat stimulation are tested. The proposed method is evaluated on a humanoid robot covered by robot skins. We also examined whether the proposed method can reproduce the desired human-like features. The proposed neuromorphic model is implemented in C++ using the Robot Operating System (ROS).

A. Response to simulated stimulation

A minimal network that contains three sensory neurons and one interneuron was trained for a single robot skin cell as described in II-C.

Multiple noxious step stimulation (15) of different intensities are applied to test the response of the proposed network. The NWR threshold for step stimulation is 44 °C.

As shown in Fig. 4, Δt decreases as the stimulation intensity increases. Consequently, the reflex gain g_R increases approximately exponentially, which is consistent with the strength of NWR evoked by radiant heat in the forearm [23].

We also apply stimulation with different baseline temperatures and heating rates to the model. Fig. 5 shows that the NWR threshold of the proposed model hardly changes with the adaptation temperature in the innoxious range, which is consistent with studies in humans [26]. In this figure, we also show that higher heating rates slightly increase the threshold, which is consistent with studies in animals [27].

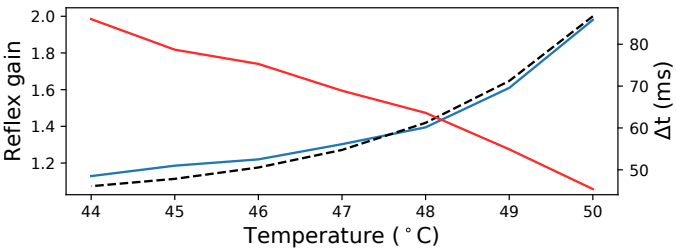

Fig. 4: The red and blue lines illustrate how the relative spike latency Δt and reflex gain g_R vary with stimulation intensity, respectively. The dashed line shows the form of NWR strength in the human forearm.

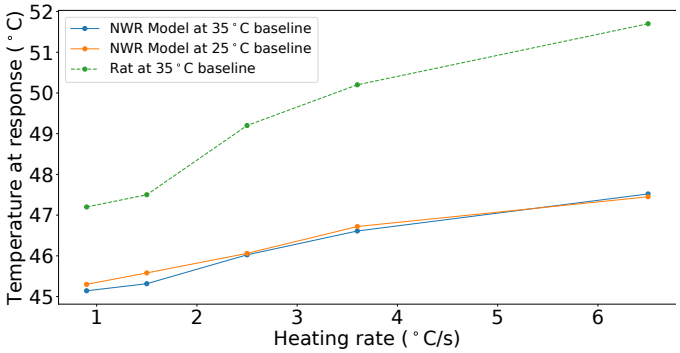

Fig. 5: NWR thresholds at different heating rates and adaptation temperatures. In comparison, The dashed line shows how the threshold at different heating rates in animals.

B. Response to heat stimulation

In this experiment, a robot skin patch with three activated skin cells is heated by a lamp of 1kW power at a ramp of about 2 °C/s with radiant heat.

Fig. 6 illustrates the records of two experiments. In the second experiment, whose results are shown in Fig. 6(b), the cell 2 and 3 were heated intensively. Compared to the results shown in Fig. 6(a), the sensory neurons with high T_a (neuron index 5 and 8) are recruited under high temperature to evoke the NWR.

In the five repetitions of the experiment, the average NWR threshold is stable at around 45 °C. Note that this threshold is slightly higher than the threshold under step stimulation, which reveals the temporal feature of the proposed model that it is more sensitive to rapidly changing temperatures.

C. Human-like features

The evoke of NWR in humans is not simply gated by a fixed threshold. Therefore, we examined whether the proposed neuromorphic model can reproduce several essential human-like features in this part.

1) Spatial summation effect: In humans, high-intensity stimulation or concurrent inputs from multiple sites can activate more sensory neurons and thus facilitate the NWR, known as the spatial summation (SS) effect [7].

The SS effect under high-intensity stimulation can be revealed in the experiment result in Fig. 6 (b). The sensory neurons with high T_a are recruited to evoke the NWR when only a part of the robot skin patch is heated intensively.

To show the SS effect under concurrent inputs, we varied the number of activated skin cells without modifying any other configuration. Fig. 7 shows the results of 5 trials with 2, 3, and 4 robot skin cells. It can be seen that the threshold decreases steadily with the increase of stimulated skin area.

If ϵ is modified according to the number of activated skin cells to keep the overall excitability $E = 1$, the NWR threshold remains stable, allowing the method to be applied to sensors with higher spatial resolution.

2) Temporal summation effect: Besides the SS effect, another essential feature of NWR is the temporal summation

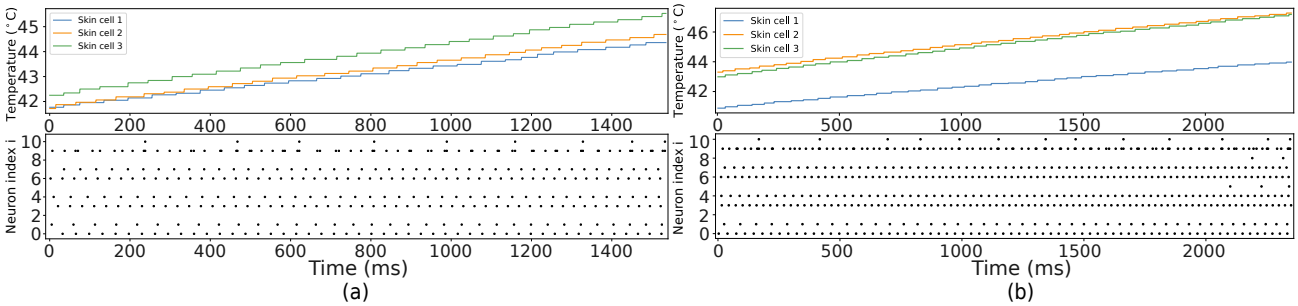

Fig. 6: The response of a network with three robot skin cells, an interneuron, and a motor neuron. (a) and (b) show the records of two trails respectively. The upper figures show the temperature of the robot skin cells, and the lower figures show the raster of the proposed SNN, where the dots denote spikes generated by the corresponding neuron.

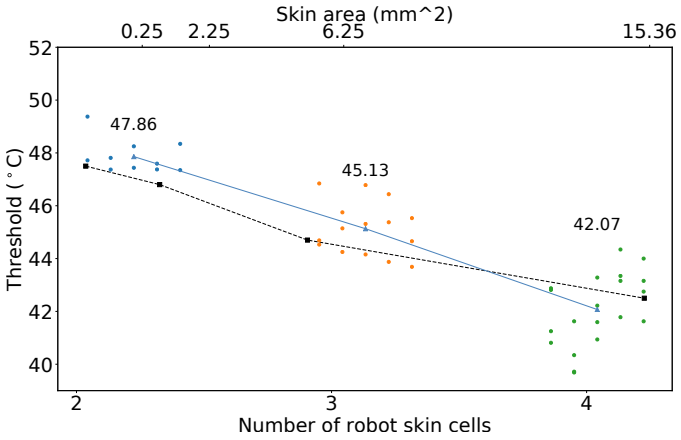

Fig. 7: SS effect experiment result. The dots in a column represent the heat pain threshold of skin cells in a trail. The values above represent the average threshold of five trials. The dashed line shows how the threshold varies with the change of affected skin area in humans [8].

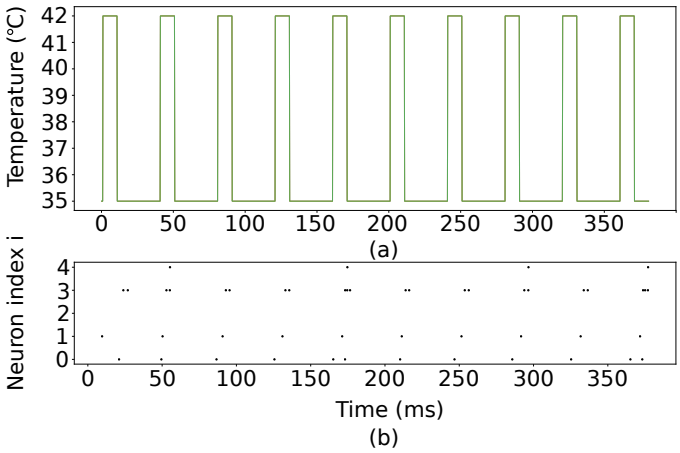

Fig. 8: TS effect experiment result. (a) shows the repeated stimulation used in the experiment. (b) shows the raster of the proposed neural network.

(TS) effect, i.e., the NWR can be evoked by high-frequency stimulation with a sub-threshold intensity [9].

In this experiment, step stimulation repeated at 25 Hz with a sub-threshold intensity is applied to the network. In each period, the stimulation phase lasts for 10 ms and returns to the baseline temperature of 35 °C afterward.

We found that the NWR threshold is lowered to 42 °C for the repeated stimulation, although the average intensity over time is significantly lower. Comparing to the results in III-A, we can find that the NWR is facilitated, which is consistent with the results of the study in human [9]. The applied stimulation and the raster of the proposed neural network are shown in Fig. 8.

D. Nociceptive withdrawal reflex in a humanoid robot

We evaluated the proposed method in a full-size humanoid robot covered with robot skin in a cooking scenario.

The humanoid robot moved its right hand along a predetermined trajectory above a working electrical stove. The temperature on the surface of the electric stove is about 220°C. The temperature information from the six activated robot skin cells on the dorsal side of the hand is processed online by the neuromorphic model under a facilitated setting.

The proposed heat-evoked NWR model can successfully detect noxious stimulations in multiple repeated experiments. Fig. 9 illustrates the movement of the humanoid robot in one of these experiments. When a noxious stimulation was detected, the robot withdrew its hand perpendicular to the skin surface away from the stimulation site while the other controllers, e.g., the self-collision avoidance and the balance controllers, were still working properly.

The recording of one of these experiments is illustrated in Fig. 10. We set $E = 1.5$ to lower the reflex threshold to avoid any potential damage to the robot. It can be observed that the humanoid robot successfully avoided the further increase of the skin surface temperature by means of NWR.

To compare the trajectories in the NWR of the humanoid robot and humans, we set the initial posture and stimulation location of the robot as in [28]. The trajectories of the forearm are illustrated in Fig. 11, and we find that their trajectories are similar. Fig. 12 shows that the proposed method allows the robot to make different responses depending on its posture and the stimulation site.

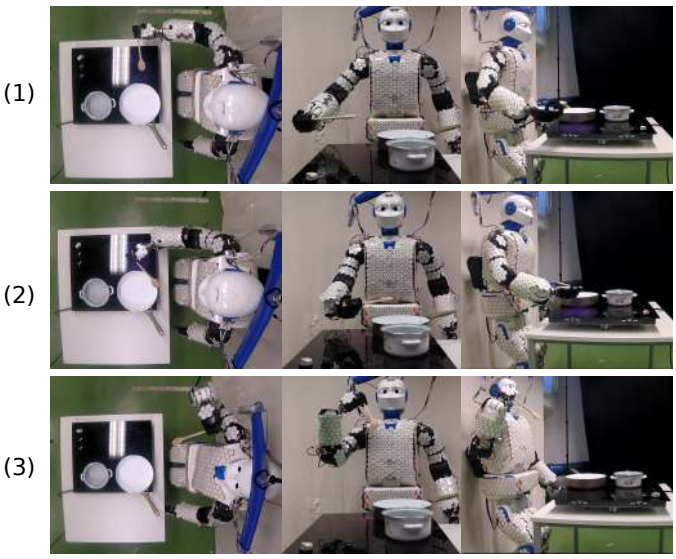

Fig. 9: NWR experiment on H1 humanoid robot. (1) shows the initial setup for the experiment. (2) shows the robot moving its hand toward the heat source. (3) shows the nociceptive withdrawal reflex evoked by the heat.

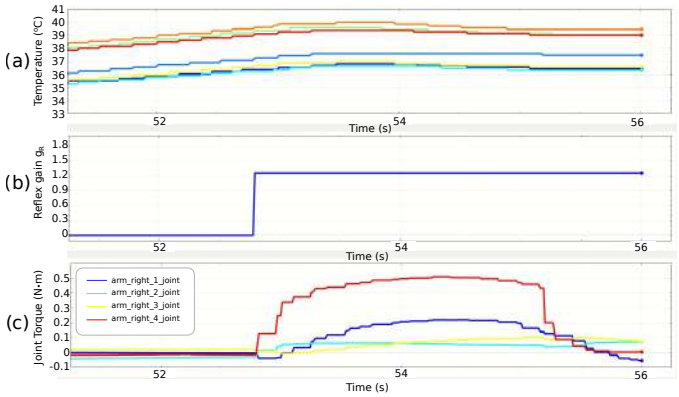

Fig. 10: (a) shows the temperature acquired from the robot skin mounted on the dorsal side of the robot hand. (b) shows the reflex gain g_R. (c) shows the joint velocity of the right arm of the humanoid robot.

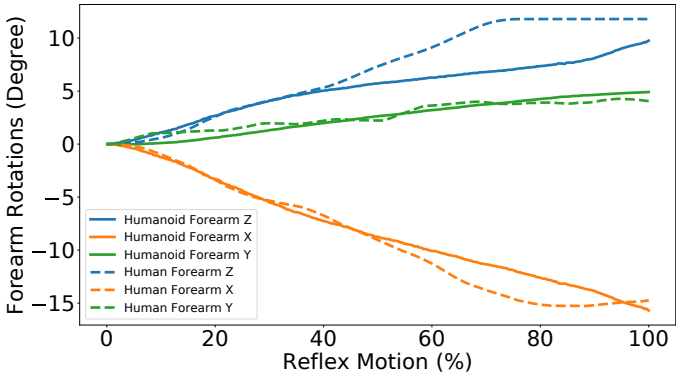

Fig. 11: Comparison of the trajectory of humanoid robots and humans forearms [28] in the NWR. The duration has been normalized due to the different speeds of a human and the humanoid robot.

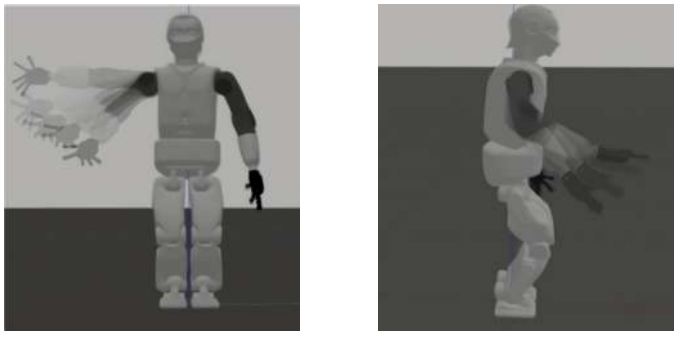

Fig. 12: (a) and (b) show the trajectories of the H1 humanoid robot in the NWR evoked in different posture. In (a) and (b), the stimulation are applied to the lateral forearm and the anterior upper arm, respectively.

E. Comparison

We compare the proposed method with the feed-forward spiking neuron (FSN) model in [1] and the neural classifier in [29]. Regarding biological plausibility, the proposed method has a structure that mimics the polysynaptic reflex arc and the encoding scheme of a population of heat sensory neurons and interneurons. On the other hand, the FSN also has a polysynaptic reflex arc structure but only mimics the encoding scheme of an individual sensory neuron. The lack of a training algorithm makes the model relies on manually tuned parameters.

We demonstrate in III-C that the proposed heat-evoked NWR model can reproduce the human-like SS and TS effects. As a comparison, we reproduced the FSN in [1], which also has a multi-layer spiking neuron structure. The FSN has the potential to reproduce the TS effect, but it is limited by the oversimplified LIF model used for the interneuron. Moreover, the lack of proper connections between the interneuron and the multiple sensory neurons inhibits the FSN from reproducing the SS effect.

The neural classifier in [29] has two perceptrons. It distinguishes between noxious and innoxious stimulation according to the intensity rather than spatial or temporal features. Therefore, it was not designed to reproduce TS or SS effect.

Both baseline methods can only make a binary classification between noxious and innocuous stimulation. In contrast, the proposed method can generate reflex strength according to the intensity of the stimulation. The humanoid robot can make the NWR according to the intensity of the stimulation and the spatial relationship between the simulation site rather than making stereotyped movement as in [1]. The neuromorphic implementation can be deployed on low-power neuromorphic hardware, which is not possible for conventional approaches, e.g., threshold with feature extraction or other post-processing. The comparison is summarized in table II.

IV. Conclusion

In this paper, we present an approach to generate the heat-evoked NWR in the upper limb of a humanoid robot. The bio-plausibility and the reproduction of essential human-like

TABLE II: Comparison between the proposed method and baseline methods.

	Bio-plausibility	SS	TS	Reflex strength	Reflex Movement
Heat-evoked NWR	Structure pf the poly-synaptic reflex arc Encoding scheme of neurons at individual and population levels	Yes	Yes	Adaptive	Adaptive
FSN	Structure pf the poly-synaptic reflex arc Encoding scheme of individual sensory neurons	No	Potentially	Fixed	Fixed
Neural classifier	No	No	No	Fixed	-

features in NWR make it possible to apply the method on neural prosthesis to provide feedback to users.

We utilize a three-layered SNN structure to mimic the poly-synaptic reflex arc in humans. The sensory neurons convert the input of the sensor data stream from the robot skin into spike trains at the population level by mimicking the encoding scheme in humans. Spike trains from multiple sensory neurons converge in the interneurons. The proper response is learned by the bio-plausible R-STDP algorithm. The motor neurons generate proper NWR strength encoded in relative spike latency. The NWR controller allows the robot to make a human-like reaction according to the site and intensity of the stimulation to avoid potential damage.

We evaluated the proposed method with simulated stimulation and radiant heat stimulation. The experimental results show that the method can robustly detect noxious heat stimulation online. Furthermore, by taking advantage of the intrinsic characteristics of the bio-mimetic method, essential features of the NWR in humans, e.g., the TS effect and the SS effect, are reproduced without additional effort.

Future researches include constructing a neuromorphic model that directly receives the raw sensor data stream and integrating the proposed sensory mechanism into a neuromorphic control architecture to create a low-power and low-latency robot protection mechanism.

REFERENCES

[1] L. E. Osborn, A. Dragomir, J. L. Betthauser, C. L. Hunt, H. H. Nguyen, R. R. Kaliki, and N. V. Thakor, "Prosthesis with neuromorphic multilayered e-dermis perceives touch and pain," *Science Robotics*, vol. 3, p. eaat3818, June 2018.

[2] G. Cheng, E. Dean-Leon, F. Bergner, J. Rogelio Guadarrama Olvera, Q. Leboutet, and P. Mittendorfer, "A Comprehensive Realization of Robot Skin: Sensors, Sensing, Control, and Applications," *Proceedings of the IEEE*, vol. 107, no. 10, pp. 2034–2051, 2019.

[3] M. Davies, N. Srinivasa, T.-H. Lin, G. Chinya, Y. Cao, S. H. Choday, G. Dimou, P. Joshi, N. Imam, S. Jain, *et al.*, "Loihi: A neuromorphic manycore processor with on-chip learning," *Ieee Micro*, vol. 38, no. 1, pp. 82–99, 2018.

[4] J. Schouenborg and H.-R. Weng, "Sensorimotor transformation in a spinal motor system," *Exp. Brain Res.*, vol. 100, July 1994.

[5] S. Rietdyk and A. Patla, "Context-dependent reflex control: some insights into the role of balance," *Exp. Brain Res.*, vol. 119, no. 2, pp. 251–259, 1998.

[6] F. Wang, E. Bélanger, S. L. Côté, P. Desrosiers, S. A. Prescott, D. C. Côté, and Y. De Koninck, "Sensory Afferents Use Different Coding Strategies for Heat and Cold," *Cell Reports*, vol. 23, pp. 2001–2013, May 2018.

[7] O. K. Andersen, "Studies of the organization of the human nociceptive withdrawal reflex.: Focus on sensory convergence and stimulation site dependency," *Acta Physiologica*, vol. 189, pp. 1–35, Apr. 2007.

[8] R. Defrin and G. Urca, "Spatial summation of heat pain: a reassessment," *Pain*, vol. 66, no. 1, pp. 23–29, 1996.

[9] L. Arendt-Nielsen, F. A. Sonnenborg, and O. K. Andersen, "Facilitation of the withdrawal reflex by repeated transcutaneous electrical stimulation: an experimental study on central integration in humans," *Eur. J. Appl. Physiol*, vol. 81, no. 3, pp. 165–173, 2000.

[10] J. Schouenborg, "Somatosensory imprinting in spinal reflex modules," *Journal of Rehabilitation Medicine*, vol. 35, pp. 73–80, Oct. 2003.

[11] G. Orchard, E. P. Frady, D. B. D. Rubin, S. Sanborn, S. B. Shrestha, F. T. Sommer, and M. Davies, "Efficient neuromorphic signal processing with loihi 2," in *2021 IEEE Workshop on Signal Processing Systems (SiPS)*, pp. 254–259, IEEE, 2021.

[12] A. L. Hodgkin and A. F. Huxley, "A quantitative description of membrane current and its application to conduction and excitation in nerve," *The Journal of physiology*, vol. 117, no. 4, p. 500, 1952.

[13] E. Izhikevich, "Which Model to Use for Cortical Spiking Neurons?," *IEEE trans. neural netw.*, vol. 15, pp. 1063–1070, Sept. 2004.

[14] G. Cheng, S. K. Ehrlich, M. Lebedev, and M. A. L. Nicolelis, "Neuroengineering challenges of fusing robotics and neuroscience," *Science Robotics*, 2020.

[15] E. Dean-Leon, J. R. Guadarrama-Olvera, F. Bergner, and G. Cheng, "Whole-body active compliance control for humanoid robots with robot skin," in *Int. Conf. Robot. Autom.*, pp. 5404–5410, 2019.

[16] E. Izhikevich, "Simple model of spiking neurons," *IEEE Transactions on Neural Networks*, vol. 14, pp. 1569–1572, Nov. 2003.

[17] F. Konietzny and H. Hensel, "The dynamic response of warm units in human skin nerves," *Pflügers Archiv*, vol. 370, no. 1, pp. 111–114, 1977.

[18] I. Darian-Smith, K. O. Johnson, C. LaMotte, Y. Shigenaga, P. Kenins, and P. Champness, "Warm fibers innervating palmar and digital skin of the monkey: responses to thermal stimuli," *Journal of Neurophysiology*, vol. 42, pp. 1297–1315, Sept. 1979.

[19] T. Takei, J. Confais, S. Tomatsu, T. Oya, and K. Seki, "Neural basis for hand muscle synergies in the primate spinal cord," *Proc. Natl. Acad. Sci. U. S. A.*, vol. 114, pp. 8643–8648, Aug. 2017.

[20] E. M. Izhikevich, "Solving the Distal Reward Problem through Linkage of STDP and Dopamine Signaling," *Cerebral Cortex*, vol. 17, pp. 2443–2452, Oct. 2007.

[21] J. C. Willer, "Comparative study of perceived pain and nociceptive flexion reflex in man," *Pain*, vol. 3, no. 1, pp. 69–80, 1977.

[22] J. C. Miller, F. Boureau, and D. Albe-Fessard, "Supraspinal influences on nociceptive flexion reflex and pain sensation in man," *Brain research*, vol. 179, no. 1, pp. 61–68, 1979.

[23] I. G. Campbell, E. Carstens, and L. R. Watkins, "Comparison of human pain sensation and flexion withdrawal evoked by noxious radiant heat," *Pain*, vol. 45, pp. 259–268, June 1991.

[24] A. Dietrich, C. Ott, and A. Albu-Schäffer, "An overview of null space projections for redundant, torque-controlled robots," *The International Journal of Robotics Research*, vol. 34, no. 11, pp. 1385–1400, 2015.

[25] L. Sentis and O. Khatib, "Synthesis of whole-body behaviors through hierarchical control of behavioral primitives," *International Journal of Humanoid Robotics*, vol. 2, no. 04, pp. 505–518, 2005.

[26] D. Le Bars, L. Villanueva, D. Bouhassira, and J. Wilier, "Diffuse noxious inhibitory controls (dnic) in animals and in man," *Acupuncture in Medicine*, vol. 9, no. 2, pp. 47–56, 1991.

[27] D. C. Yeomans and H. K. Proudfit, "Characterization of the foot withdrawal response to noxious radiant heat in the rat," *Pain*, vol. 59, no. 1, pp. 85–94, 1994.

[28] T. S. Dahl, E. A. Swere, and A. Palmer, "Touch-triggered withdrawal reflexes for safer robots," *New frontiers in human-robot interaction*, pp. 281–304, 2011.

[29] J. Neto, R. Chirila, A. S. Dahiya, A. Christou, D. Shakthivel, and R. Dahiya, "Skin-Inspired Thermoreceptors-Based Electronic Skin for Biomimicking Thermal Pain Reflexes," *Advanced Science*, vol. 9, p. 2201525, Sept. 2022.